

67. CP Violation in K_L Decays

Updated April 2016 by L. Wolfenstein (Carnegie-Mellon University), C.-J. Lin (LBNL), and T.G. Trippe (LBNL).

The symmetries C (particle-antiparticle interchange) and P (space inversion) hold for strong and electromagnetic interactions. After the discovery of large C and P violation in the weak interactions, it appeared that the product CP was a good symmetry. In 1964 CP violation was observed in K^0 decays at a level given by the parameter $\epsilon \approx 2.3 \times 10^{-3}$.

A unified treatment of CP violation in K , D , B , and B_s mesons is given in “ CP Violation in Meson Decays” by D. Kirkby and Y. Nir in this *Review*. A more detailed review including a thorough discussion of the experimental techniques used to determine CP violation parameters is given in a book by K. Kleinknecht [1]. Here we give a concise summary of the formalism needed to define the parameters of CP violation in K_L decays, and a description of our fits for the best values of these parameters.

67.1. Formalism for CP violation in Kaon decay

CP violation has been observed in the semi-leptonic decays $K_L^0 \rightarrow \pi^\mp \ell^\pm \nu$, and in the nonleptonic decay $K_L^0 \rightarrow 2\pi$. The experimental numbers that have been measured are

$$A_L = \frac{\Gamma(K_L^0 \rightarrow \pi^- \ell^+ \nu) - \Gamma(K_L^0 \rightarrow \pi^+ \ell^- \nu)}{\Gamma(K_L^0 \rightarrow \pi^- \ell^+ \nu) + \Gamma(K_L^0 \rightarrow \pi^+ \ell^- \nu)} \quad (67.1a)$$

$$\begin{aligned} \eta_{+-} &= A(K_L^0 \rightarrow \pi^+ \pi^-) / A(K_S^0 \rightarrow \pi^+ \pi^-) \\ &= |\eta_{+-}| e^{i\phi_{+-}} \end{aligned} \quad (67.1b)$$

$$\begin{aligned} \eta_{00} &= A(K_L^0 \rightarrow \pi^0 \pi^0) / A(K_S^0 \rightarrow \pi^0 \pi^0) \\ &= |\eta_{00}| e^{i\phi_{00}} . \end{aligned} \quad (67.1c)$$

CP violation can occur either in the $K^0 - \bar{K}^0$ mixing or in the decay amplitudes. Assuming CPT invariance, the mass eigenstates of the $K^0 - \bar{K}^0$ system can be written

$$|K_S\rangle = p|K^0\rangle + q|\bar{K}^0\rangle, \quad |K_L\rangle = p|K^0\rangle - q|\bar{K}^0\rangle. \quad (67.2)$$

If CP invariance held, we would have $q = p$ so that K_S would be CP -even and K_L CP -odd. (We define $|\bar{K}^0\rangle$ as $CP |K^0\rangle$). CP violation in $K^0 - \bar{K}^0$ mixing is then given by the parameter $\tilde{\epsilon}$ where

$$\frac{p}{q} = \frac{(1 + \tilde{\epsilon})}{(1 - \tilde{\epsilon})}. \quad (67.3)$$

CP violation can also occur in the decay amplitudes

$$A(K^0 \rightarrow \pi\pi(I)) = A_I e^{i\delta_I}, \quad A(\bar{K}^0 \rightarrow \pi\pi(I)) = A_I^* e^{i\delta_I}, \quad (67.4)$$

where I is the isospin of $\pi\pi$, δ_I is the final-state phase shift, and A_I would be real if CP invariance held. The CP -violating observables are usually expressed in terms of ϵ and ϵ' defined by

$$\eta_{+-} = \epsilon + \epsilon', \quad \eta_{00} = \epsilon - 2\epsilon'. \quad (67.5a)$$

One can then show [2]

$$\epsilon = \tilde{\epsilon} + i (\text{Im } A_0 / \text{Re } A_0), \quad (67.5b)$$

2 67. *CP* violation in K_L decays

$$\sqrt{2}\epsilon' = ie^{i(\delta_2 - \delta_0)}(\text{Re } A_2/\text{Re } A_0) (\text{Im } A_2/\text{Re } A_2 - \text{Im } A_0/\text{Re } A_0) , \quad (67.5c)$$

$$A_L = 2\text{Re } \epsilon/(1 + |\epsilon|^2) \approx 2\text{Re } \epsilon . \quad (67.5d)$$

In Eqs. (67.5a), small corrections [3] of order $\epsilon' \times \text{Re } (A_2/A_0)$ are neglected, and Eq. (67.5d) assumes the $\Delta S = \Delta Q$ rule.

The quantities $\text{Im } A_0$, $\text{Im } A_2$, and $\text{Im } \tilde{\epsilon}$ depend on the choice of phase convention, since one can change the phases of K^0 and \bar{K}^0 by a transformation of the strange quark state $|s\rangle \rightarrow |s\rangle e^{i\alpha}$; of course, observables are unchanged. It is possible by a choice of phase convention to set $\text{Im } A_0$ or $\text{Im } A_2$ or $\text{Im } \tilde{\epsilon}$ to zero, but none of these is zero with the usual phase conventions in the Standard Model. The choice $\text{Im } A_0 = 0$ is called the Wu-Yang phase convention [4], in which case $\epsilon = \tilde{\epsilon}$. The value of ϵ' is independent of phase convention, and a nonzero value demonstrates *CP* violation in the decay amplitudes, referred to as direct *CP* violation. The possibility that direct *CP* violation is essentially zero, and that *CP* violation occurs only in the mixing matrix, was referred to as the superweak theory [5].

By applying *CPT* invariance and unitarity the phase of ϵ is given approximately by

$$\phi_\epsilon \approx \tan^{-1} \frac{2(m_{K_L} - m_{K_S})}{\Gamma_{K_S} - \Gamma_{K_L}} \approx 43.52 \pm 0.05^\circ , \quad (67.6a)$$

while Eq. (67.5c) gives the phase of ϵ' to be

$$\phi_{\epsilon'} = \delta_2 - \delta_0 + \frac{\pi}{2} \approx 42.3 \pm 1.5^\circ , \quad (67.6b)$$

where the numerical value is based on an analysis of $\pi\text{-}\pi$ scattering using chiral perturbation theory [6]. The approximation in Eq. (67.6a) depends on the assumption that direct *CP* violation is very small in all K^0 decays. This is expected to be good to a few tenths of a degree, as indicated by the small value of ϵ' and of η_{+-0} and η_{000} , the *CP*-violation parameters in the decays $K_S \rightarrow \pi^+\pi^-\pi^0$ [7], and $K_S \rightarrow \pi^0\pi^0\pi^0$ [8]. The relation in Eq. (67.6a) is exact in the superweak theory, so this is sometimes called the superweak-phase ϕ_{SW} . An important point for the analysis is that $\cos(\phi_{\epsilon'} - \phi_\epsilon) \simeq 1$. The consequence is that only two real quantities need be measured, the magnitude of ϵ and the value of (ϵ'/ϵ) , including its sign. The measured quantity $|\eta_{00}/\eta_{+-}|^2$ is very close to unity so that we can write

$$|\eta_{00}/\eta_{+-}|^2 \approx 1 - 6\text{Re } (\epsilon'/\epsilon) \approx 1 - 6\epsilon'/\epsilon , \quad (67.7a)$$

$$\text{Re}(\epsilon'/\epsilon) \approx \frac{1}{3}(1 - |\eta_{00}/\eta_{+-}|) . \quad (67.7b)$$

From the experimental measurements in this edition of the *Review*, and the fits discussed in the next section, one finds

$$|\epsilon| = (2.228 \pm 0.011) \times 10^{-3} , \quad (67.8a)$$

$$\phi_\epsilon = (43.5 \pm 0.5)^\circ, \quad (67.8b)$$

$$\text{Re}(\epsilon'/\epsilon) \approx \epsilon'/\epsilon = (1.66 \pm 0.23) \times 10^{-3}, \quad (67.8c)$$

$$\phi_{+-} = (43.4 \pm 0.5)^\circ, \quad (67.8d)$$

$$\phi_{00} - \phi_{+-} = (0.34 \pm 0.32)^\circ, \quad (67.8e)$$

$$A_L = (3.32 \pm 0.06) \times 10^{-3}. \quad (67.8f)$$

Direct *CP* violation, as indicated by ϵ'/ϵ , is expected in the Standard Model. However, the numerical value cannot be reliably predicted because of theoretical uncertainties [9]. The value of A_L agrees with Eq. (67.5d). The values of ϕ_{+-} and $\phi_{00} - \phi_{+-}$ are used to set limits on *CPT* violation [see “Tests of Conservation Laws”].

67.2. Fits for K_L^0 *CP*-violation parameters

In recent years, K_L^0 *CP*-violation experiments have improved our knowledge of *CP*-violation parameters, and their consistency with the expectations of *CPT* invariance and unitarity. To determine the best values of the *CP*-violation parameters in $K_L^0 \rightarrow \pi^+\pi^-$ and $\pi^0\pi^0$ decay, we make two types of fits, one for the phases ϕ_{+-} and ϕ_{00} jointly with Δm and τ_S , and the other for the amplitudes $|\eta_{+-}|$ and $|\eta_{00}|$ jointly with the $K_L^0 \rightarrow \pi\pi$ branching fractions.

67.2.1. Fits to ϕ_{+-} , ϕ_{00} , $\Delta\phi$, Δm , and τ_S data :

These are joint fits to the data on ϕ_{+-} , ϕ_{00} , the phase difference $\Delta\phi = \phi_{00} - \phi_{+-}$, the $K_L^0 - K_S^0$ mass difference Δm , and the K_S^0 mean life τ_S , including the effects of correlations.

Measurements of ϕ_{+-} and ϕ_{00} are highly correlated with Δm and τ_S . Some measurements of τ_S are correlated with Δm . The correlations are given in the footnotes of the ϕ_{+-} and ϕ_{00} sections of the K_L^0 Listings, and the τ_S section of the K_S^0 Listings.

In most cases, the correlations are quoted as 100%, *i.e.*, with the value and error of ϕ_{+-} or ϕ_{00} given at a fixed value of Δm and τ_S , with additional terms specifying the dependence of the value on Δm and τ_S . These cases lead to diagonal bands in Figs. 67.1 and 67.2. The KTeV experiment [10] quotes its results as values of Δm , τ_S , ϕ_ϵ , $\text{Re}(\epsilon'/\epsilon)$, and $\text{Im}(\epsilon'/\epsilon)$ with correlations, leading to the ellipses labeled “b.” The correlations for the KTeV measurements are given in the $\text{Im}(\epsilon'/\epsilon)$ section of the K_L^0 Listings. For small $|\epsilon'/\epsilon|$, $\phi_{+-} \approx \phi_\epsilon + \text{Im}(\epsilon'/\epsilon)$.

The data on τ_S , Δm , and ϕ_{+-} shown in Figs. 67.1 and 67.2 are combined with data on ϕ_{00} and $\phi_{00} - \phi_{+-}$ in two fits, one without assuming *CPT*, and the other with this assumption. The results without assuming *CPT* are shown as ellipses labeled “a.” These ellipses are seen to be in good agreement with the superweak phase

$$\phi_{\text{SW}} = \tan^{-1} \left(\frac{2\Delta m}{\Delta\Gamma} \right) = \tan^{-1} \left(\frac{2\Delta m \tau_S \tau_L}{\hbar(\tau_L - \tau_S)} \right). \quad (67.9)$$

In Figs. 67.1 and 67.2, ϕ_{SW} is shown as narrow bands labeled “j.”

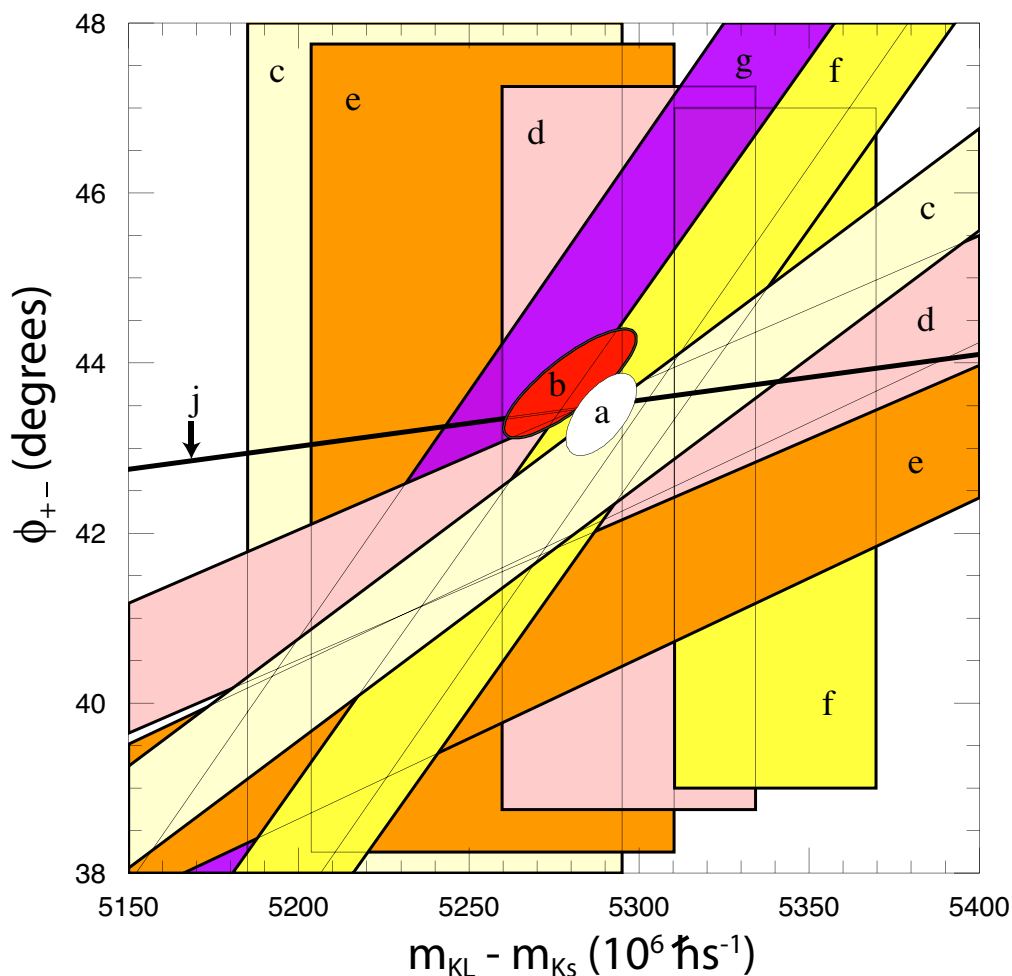


Figure 67.1: ϕ_{+-} vs Δm for experiments which do not assume CPT invariance. Δm measurements appear as vertical bands spanning $\Delta m \pm 1\sigma$, cut near the top and bottom to aid the eye. Most ϕ_{+-} measurements appear as diagonal bands spanning $\phi_{+-} \pm \sigma_\phi$. Data are labeled by letters: “b”–FNAL KTeV, “c”–CERN CPLEAR, “d”–FNAL E773, “e”–FNAL E731, “f”–CERN, “g”–CERN NA31, and are cited in Table 67.1. The narrow band “j” shows ϕ_{SW} . The ellipse “a” shows the $\chi^2 = 1$ contour of the fit result.

Table 67.2 column 2, “Fit w/o CPT ,” gives the resulting fitted parameters, while Table 67.3 gives the correlation matrix for this fit. The white ellipses labeled “a” in Fig. 67.1 and Fig. 67.2 are the $\chi^2 = 1$ contours for this fit.

For experiments which have dependencies on unseen fit parameters, that is, parameters other than those shown on the x or y axis of the figure, their band positions are evaluated using the fit results and their band widths include the fitted uncertainty in the unseen parameters. This is also true for the ϕ_{SW} bands.

If CPT invariance and unitarity are assumed, then by Eq. (67.6a), the phase of ϵ is

Table 67.1: References, Document ID's, and sources corresponding to the letter labels in the figures. The data are given in the ϕ_{+-} and Δm sections of the K_L Listings, and the τ_S section of the K_S Listings.

Label	Source	PDG Document ID	Ref.
a	this <i>Review</i>	OUR FIT	
b	FNAL KTeV	ABOUZAID 11	[10]
c	CERN CPLEAR	APOSTOLAKIS 99C	[11]
d	FNAL E773	SCHWINGENHEUER 95	[12]
e	FNAL E731	GIBBONS 93,93C	[13,14]
f	CERN	GEWENIGER 74B,74C	[15,16]
g	CERN NA31	CAROSI 90	[17]
h	CERN NA48	LAI 02C	[18]
i	CERN NA31	BERTANZA 97	[19]
j	this <i>Review</i>	SUPERWEAK 16	

constrained to be approximately equal to

$$\phi_{\text{SW}} = (43.50258 \pm 0.00021)^\circ + 54.1(\Delta m - 0.5289)^\circ + 32.0(\tau_S - 0.89564) \quad (67.10)$$

where we have linearized the Δm and τ_S dependence of Eq. (67.9). The error ± 0.00021 is due to the uncertainty in τ_L . Here Δm has units $10^{10} \hbar s^{-1}$ and τ_S has units 10^{-10} s.

If in addition we use the observation that $Re(\epsilon'/\epsilon) \ll 1$ and $\cos(\phi_{\epsilon'} - \phi_\epsilon) \simeq 1$, as well as the numerical value of $\phi_{\epsilon'}$ given in Eq. (67.6b), then Eqs. (67.5a), which are sketched in Fig. 67.3, lead to the constraint

$$\begin{aligned} \phi_{00} - \phi_{+-} &\approx -3 \operatorname{Im} \left(\frac{\epsilon'}{\epsilon} \right) \\ &\approx -3 \operatorname{Re} \left(\frac{\epsilon'}{\epsilon} \right) \tan(\phi_{\epsilon'} - \phi_\epsilon) \\ &\approx 0.006^\circ \pm 0.008^\circ, \end{aligned} \quad (67.11)$$

so that $\phi_{+-} \approx \phi_{00} \approx \phi_\epsilon \approx \phi_{\text{SW}}$.

In the fit assuming *CPT*, we constrain $\phi_\epsilon = \phi_{\text{SW}}$ using the linear expression in Eq. (67.10), and constrain $\phi_{00} - \phi_{+-}$ using Eq. (67.11). These constraints are inserted into the Listings with the Document ID of SUPERWEAK 16. Some additional data for which the authors assumed *CPT* are added to this fit or substitute for other less precise data for which the authors did not make this assumption. See the Listings for details.

The results of this fit are shown in Table 67.2, column 3, “Fit w/*CPT*,” and the correlation matrix is shown in Table 67.4. The Δm precision is improved by the *CPT* assumption.

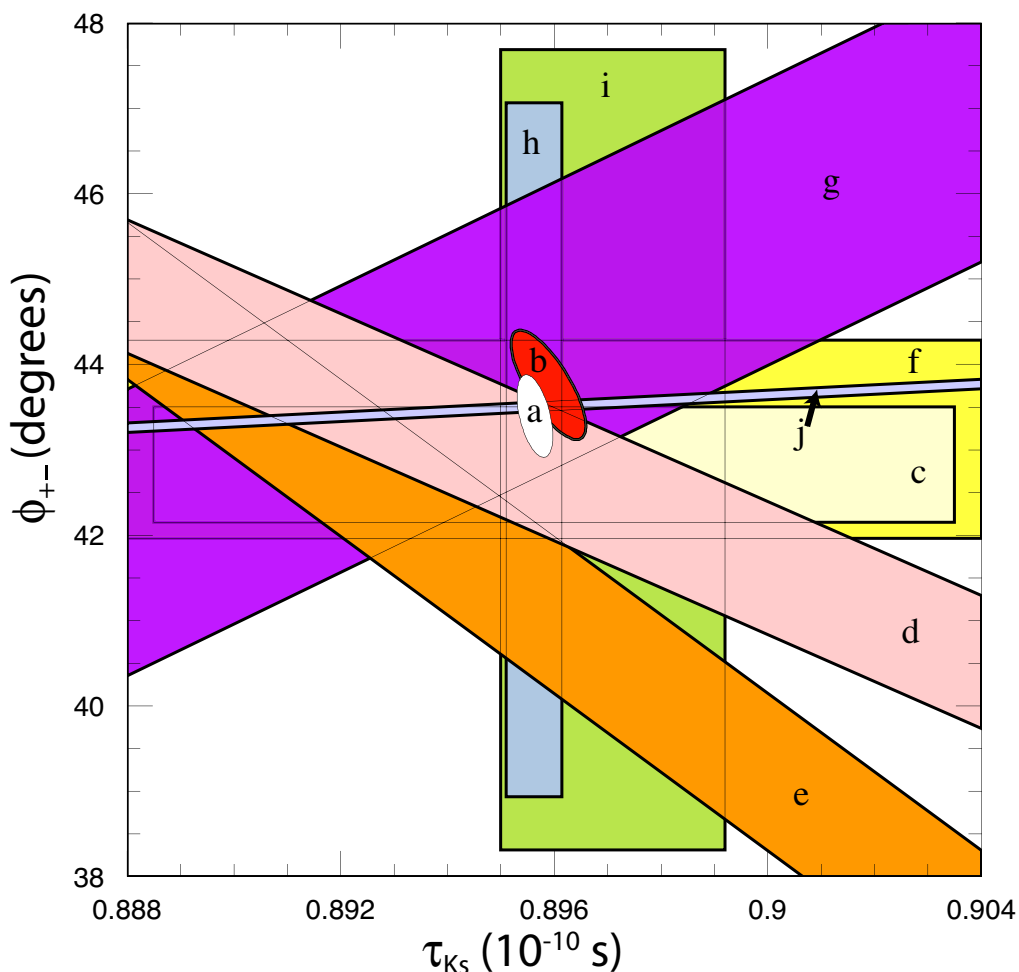


Figure 67.2: ϕ_{+-} vs τ_S . τ_S measurements appear as vertical bands spanning $\tau_S \pm 1\sigma$, some of which are cut near the top and bottom to aid the eye. Most ϕ_{+-} measurements appear as diagonal or horizontal bands spanning $\phi_{+-} \pm \sigma_\phi$. Data are labeled by letters: “b”–FNAL KTeV, “c”–CERN CPLEAR, “d”–FNAL E773, “e”–FNAL E731, “f”–CERN, “g”–CERN NA31, “h”–CERN NA48, “i”–CERN NA31, and are cited in Table 67.1. The narrow band “j” shows ϕ_{SW} . The ellipse “a” shows the fit result’s $\chi^2 = 1$ contour.

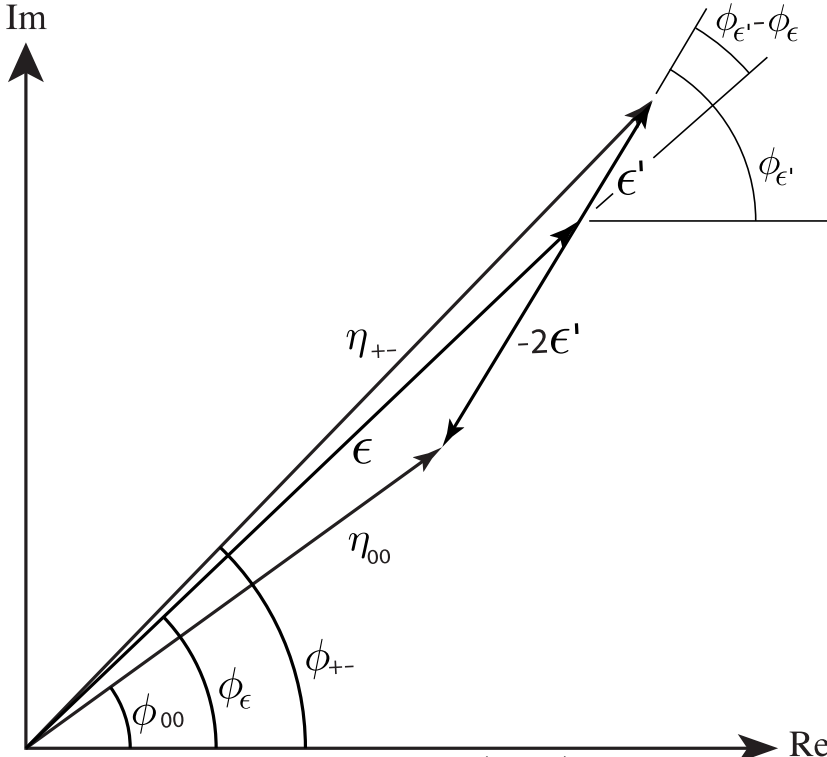
67.2.2. Fits for ϵ'/ϵ , $|\eta_{+-}|$, $|\eta_{00}|$, and $B(K_L \rightarrow \pi\pi)$:

We list measurements of $|\eta_{+-}|$, $|\eta_{00}|$, $|\eta_{00}/\eta_{+-}|$, and ϵ'/ϵ . Independent information on $|\eta_{+-}|$ and $|\eta_{00}|$ can be obtained from measurements of the K_L^0 and K_S^0 lifetimes (τ_L , τ_S), and branching ratios (B) to $\pi\pi$, using the relations

$$|\eta_{+-}| = \left[\frac{B(K_L^0 \rightarrow \pi^+\pi^-)}{\tau_L} \frac{\tau_S}{B(K_S^0 \rightarrow \pi^+\pi^-)} \right]^{1/2}, \quad (67.12a)$$

Table 67.2: Fit results for ϕ_{+-} , Δm , τ_S , ϕ_{00} , $\Delta\phi = \phi_{00} - \phi_{+-}$, and ϕ_ϵ without and with the *CPT* assumption.

Quantity(units)	Fit w/o <i>CPT</i>	Fit w/ <i>CPT</i>
$\phi_{+-}(\circ)$	43.4 ± 0.5 (S=1.2)	43.51 ± 0.05 (S=1.2)
$\Delta m(10^{10}\hbar s^{-1})$	0.5289 ± 0.0010	0.5293 ± 0.0009 (S=1.3)
$\tau_S(10^{-10}s)$	0.89564 ± 0.00033	0.8954 ± 0.0004 (S=1.1)
$\phi_{00}(\circ)$	43.7 ± 0.6 (S=1.2)	43.52 ± 0.05 (S=1.3)
$\Delta\phi(\circ)$	0.34 ± 0.32	0.006 ± 0.014 (S=1.7)
$\phi_\epsilon(\circ)$	43.5 ± 0.5 (S=1.3)	43.52 ± 0.05 (S=1.2)
χ^2	16.4	20.0
# Deg. Free.	14	16


Figure 67.3: Sketch of Eqs. (67.5a). Not to scale.

$$|\eta_{00}| = \left[\frac{B(K_L^0 \rightarrow \pi^0\pi^0)}{\tau_L} \frac{\tau_S}{B(K_S^0 \rightarrow \pi^0\pi^0)} \right]^{1/2}. \quad (67.12b)$$

For historical reasons, the branching ratio fits and the *CP*-violation fits are done

Table 67.3: Correlation matrix for the results of the fit without the *CPT* assumption

	ϕ_{+-}	Δm	τ_S	ϕ_{00}	$\Delta\phi$	ϕ_ϵ
ϕ_{+-}	1.000	0.596	-0.488	0.827	-0.040	0.976
Δm	0.596	1.000	-0.572	0.487	-0.035	0.580
τ_S	-0.488	-0.572	1.000	-0.423	-0.014	-0.484
ϕ_{00}	0.827	0.487	-0.423	1.000	0.529	0.929
$\Delta\phi$	-0.040	-0.035	-0.014	0.529	1.000	0.178
ϕ_ϵ	0.976	0.580	-0.484	0.929	0.178	1.000

Table 67.4: Correlation matrix for the results of the fit with the *CPT* assumption

	ϕ_{+-}	Δm	τ_S	ϕ_{00}	$\Delta\phi$	ϕ_ϵ
ϕ_{+-}	1.000	0.972	-0.311	0.957	-0.105	0.995
Δm	0.972	1.000	-0.509	0.958	-0.007	0.977
τ_S	-0.311	-0.509	1.000	-0.306	0.004	-0.312
ϕ_{00}	0.957	0.958	-0.306	1.000	0.189	0.981
$\Delta\phi$	-0.105	-0.007	0.004	0.189	1.000	-0.006
ϕ_ϵ	0.995	0.977	-0.312	0.981	-0.006	1.000

separately, but we want to include the influence of $|\eta_{+-}|$, $|\eta_{00}|$, $|\eta_{00}/\eta_{+-}|$, and ϵ'/ϵ measurements on $B(K_L^0 \rightarrow \pi^+\pi^-)$ and $B(K_L^0 \rightarrow \pi^0\pi^0)$ and vice versa. We approximate a global fit to all of these measurements by first performing two independent fits: 1) BRFIT, a fit to the K_L^0 branching ratios, rates, and mean life, and 2) ETAFIT, a fit to the $|\eta_{+-}|$, $|\eta_{00}|$, $|\eta_{+-}/\eta_{00}|$, and ϵ'/ϵ measurements. The results from fit 1, along with the K_S^0 values from this edition, are used to compute values of $|\eta_{+-}|$ and $|\eta_{00}|$, which are included as measurements in the $|\eta_{00}|$ and $|\eta_{+-}|$ sections with a document ID of BRFIT 16. Thus, the fit values of $|\eta_{+-}|$ and $|\eta_{00}|$ given in this edition include both the direct measurements and the results from the branching ratio fit.

The process is reversed in order to include the direct $|\eta|$ measurements in the branching ratio fit. The results from fit 2 above (before including BRFIT 16 values) are used along with the K_L^0 and K_S^0 mean lives and the $K_S^0 \rightarrow \pi\pi$ branching fractions to compute the K_L^0 branching ratio $\Gamma(K_L^0 \rightarrow \pi^0\pi^0)/\Gamma(K_L^0 \rightarrow \pi^+\pi^-)$. This branching ratio value is included as a measurement in the branching ratio section with a document ID of ETAFIT 16. Thus, the K_L^0 branching ratio fit values in this edition include the results of the direct measurement of $|\eta_{00}/\eta_{+-}|$ and ϵ'/ϵ . Most individual measurements of $|\eta_{+-}|$ and $|\eta_{00}|$

enter our fits directly via the corresponding measurements of $\Gamma(K_L^0 \rightarrow \pi^+\pi^-)/\Gamma(\text{total})$ and $\Gamma(K_L^0 \rightarrow \pi^0\pi^0)/\Gamma(\text{total})$, and those that do not have too large errors to have any influence on the fitted values of these branching ratios. A more detailed discussion of these fits is given in the 1990 edition of this *Review* [20].

References:

1. K. Kleinknecht, "Uncovering *CP* violation: experimental clarification in the neutral *K* meson and *B* meson systems," *Springer Tracts in Modern Physics*, vol. 195 (Springer Verlag 2003).
2. B. Winstein and L. Wolfenstein, *Rev. Mod. Phys.* **65**, 1113 (1993).
3. M.S. Sozzi, *Eur. Phys. J.* **C36**, 37 (2004).
4. T.T. Wu and C.N. Yang, *Phys. Rev. Lett.* **13**, 380 (1964).
5. L. Wolfenstein, *Phys. Rev. Lett.* **13**, 562 (1964);
L. Wolfenstein, *Comm. Nucl. Part. Phys.* **21**, 275 (1994).
6. G. Colangelo, J. Gasser, and H. Leutwyler, *Nucl. Phys.* **B603**, 125 (2001).
7. R. Adler *et al.*, (CPLEAR Collab.), *Phys. Lett.* **B407**, 193 (1997);
P. Bloch, *Proceedings of Workshop on K Physics* (Orsay 1996), ed. L. Iconomidou-Fayard, Edition Frontieres, Gif-sur-Yvette, France (1997) p. 307.
8. A. Lai *et al.*, *Phys. Lett.* **B610**, 165 (2005).
9. G. Buchalla, A.J. Buras, and M.E. Lautenbacher, *Rev. Mod. Phys.* **68**, 1125 (1996);
S. Bosch *et al.*, *Nucl. Phys.* **B565**, 3 (2000);
S. Bertolini, M. Fabrichesi, and J.O. Egg, *Rev. Mod. Phys.* **72**, 65 (2000).
10. E. Abouzaid *et al.*, *Phys. Rev.* **D83**, 092001 (2011).
11. A. Apostolakis *et al.*, *Phys. Lett.* **B458**, 545 (1999).
12. B. Schwingenheuer *et al.*, *Phys. Rev. Lett.* **74**, 4376 (1995).
13. L.K. Gibbons *et al.*, *Phys. Rev. Lett.* **70**, 1199 (1993) and footnote in Ref. 12.
14. L.K. Gibbons, Thesis, RX-1487, Univ. of Chicago, 1993.
15. C. Geweniger *et al.*, *Phys. Lett.* **48B**, 487 (1974).
16. C. Geweniger *et al.*, *Phys. Lett.* **52B**, 108 (1974).
17. R. Carosi *et al.*, *Phys. Lett.* **B237**, 303 (1990).
18. A. Lai *et al.*, *Phys. Lett.* **B537**, 28 (2002).
19. L. Bertanza *et al.*, *Z. Phys.* **C73**, 629 (1997).
20. J.J. Hernandez *et al.*, Particle Data Group, *Phys. Lett.* **B239**, 1 (1990).